

DETERMINATION OF OSCILLATOR STRENGTHS FROM THE SELF-ABSORPTION OF RESONANCE RADIATION IN RARE GASES—II. NEON AND ARGON

W. B. WESTERVELD, TH. F. A. MULDER, and J. VAN ECK
Fysisch Laboratorium, Rijksuniversiteit Utrecht, Princetonplein 5, Utrecht, The Netherlands

(Received 13 November 1978)

Abstract—A previously developed method, based on the self-absorption of resonance radiation, is used to derive oscillator strengths for fourteen resonance transitions of neon and argon. Electron beam excitation of the atoms is used to produce the resonance radiation, which is partly absorbed in the gas between the beam and the spectrometer. A v.u.v. spectrometer is employed to record the radiation intensities as a function of gas pressure. Oscillator strengths are derived from the measurements by using a simple formalism. The influence of recoil effects (as a consequence of the excitation process) on the shape of the spectral emission lines and thereby on the transmission is checked by detailed numerical calculations. Special attention is paid to the determination of the quantities relevant in absorption measurements, i.e. the temperature, the absorption length and the number density of the atoms. The oscillator strengths obtained are compared with results from other experiments of various types (particularly forward inelastic electron scattering, for which on the whole good agreement with the present results exists) and from theoretical calculations.

1. INTRODUCTION

THERE is a continuously growing need of accurate atomic data in fields closely related to atomic physics such as plasmaphysics and astrophysics. The use of spectroscopic techniques in plasmaphysics, for instance, is very attractive because it is a diagnostic method which does not disturb the plasma. The interpretation of the plasma parameters in terms of these spectroscopic data is only possible with adequate knowledge of the relevant fundamental atomic data.^(1–3) The same is true for astrophysics, the more so as presently measurements are made with the help of spacecrafts so that the wavelength region of the v.u.v. can be fully covered. The need for accurate knowledge of oscillator strengths (or, equivalently, transition probabilities) is evident [see, for instance, MENZEL⁽⁴⁾]. In astrophysics, this concerns in many cases electric-dipole forbidden transitions or transitions in highly charged ions for which it is difficult to measure the oscillator strengths in the laboratory. In these cases, it is often necessary to turn to calculations; therefore, an adequate knowledge of atomic wave functions is essential. A number of semi-empirical schemes have been proposed to calculate oscillator strengths [e.g. BATES and DAMGAARD⁽⁵⁾] but the *ab initio* calculation of accurate oscillator strengths remains a difficult task. Calculated oscillator strengths are often very sensitive to small errors in the wave functions employed. Accurate results have so far been obtained only for one-electron and two-electron systems [BETHE and SALPETER⁽⁶⁾ and SCHIFF *et al.*⁽⁷⁾]. It is often difficult to judge the quality of a particular calculation on purely theoretical grounds. It has only recently become possible to calculate rigid upper and lower bounds for oscillator strengths [see WEINHOLD⁽⁸⁾ and ANDERSON and WEINHOLD⁽⁹⁾], but the calculation of tight bounds requires the use of correspondingly accurate wavefunctions. Summarizing, we may conclude that the comparison with experimental values remains of vital importance to get insight into the accuracy of calculated oscillator strengths for many-electron systems.

Experimentally, it is now possible to measure lifetimes accurately, even for excited states of highly charged ions [notably after the introduction of the beam foil technique, although cascade processes can impose problems in the interpretation; for a review, see BERRY⁽¹⁰⁾]. However, in most cases, an excited atom can make radiative transitions to more than one lower lying level and, therefore, the information obtained from lifetime measurements is not as detailed as one might wish. Clearly, it would be advantageous to have experimental methods by which oscillator strengths are obtained directly.

In the present work, we report on oscillator strengths for fourteen resonance transitions of neon and argon, measured by means of a self-absorption method. An outline of this method has been given previously [WESTERVELD and VAN ECK,⁽¹¹⁾ referred to as I]. Data for most of these transitions have so far been obtained primarily from forward inelastic scattering of high energy electrons [the derivation of oscillator strengths from electron-scattering data has been described extensively by LASSETTRE and SKERBELE⁽¹²⁾].

In short, the present experiments are carried out as follows: resonance radiation is produced in an excitation chamber (containing the gas under study) by exciting the atoms through electron impact. In this way, resonance radiation is produced with a well-known frequency distribution, i.e. a Doppler profile according to the gas temperature (complications arise when the recoil effects due to the excitation process are non-negligible or when various isotopes are present with non-negligible isotope shifts). A part of the resonance radiation is absorbed by the ground-state atoms with an absorption profile identical to the emission profile of the radiation. The attenuation of the radiation on its way through the gas from the excitation region to the entrance slit of a v.u.v. spectrometer is measured as a function of gas pressure. Under these conditions, we may express the transmitted fraction of the radiation intensity in terms of the absorption length, the absolute temperature, the number density of the atoms, and the absorption oscillator strength of the observed transition. From a comparison with experimentally determined transmission data, the absorption oscillator strength, which is the only unknown constant, is then derived.

2. ACCURACY OF OSCILLATOR STRENGTHS DERIVED FROM SELF-ABSORPTION DATA

In this section, we deal with some questions concerning the derivation of oscillator strengths from self-absorption measurements, which were not or only in part treated in I. The measuring procedure and treatment of the data have been fully described in I. We briefly recall the relevant formulae. The initial frequency distribution $I_\nu(0)$ of a beam of resonance radiation is changed into a different distribution $I_\nu(x)$ after the beam has travelled a distance x in the target gas due to absorption by ground-state atoms. Under the condition of a purely Doppler-broadened absorption line profile, the absorption coefficient $k_D(\nu)$ is given as

$$k_D(\nu) = k_0 \exp \left\{ -\frac{Mc^2}{2k_B T} [(\nu/\nu_0) - 1]^2 \right\}; \quad (1)$$

where ν_0 is the central frequency of the line, c the light velocity, k_B is the Boltzmann constant, T is the absolute temperature of the gas, M is the mass of the absorbing atoms and

$$k_0 = \frac{e^2}{(4\pi\epsilon_0)m\nu_0} \sqrt{\left(\frac{\pi M}{2k_B T}\right)} f_{ji} n(p), \quad (2)$$

where e is the electron charge, $n(p)$ is the atom number density at pressure p , ϵ_0 is the vacuum permittivity, m is the electron mass, and f_{ji} is the absorption oscillator strength.

The transmission function $G(k_0 x)$ is defined as the fraction of the line intensity transmitted over an absorption length x , consequently,

$$G(k_0 x) = \frac{\int I_\nu(0) \exp[-k(\nu)x] d\nu}{\int I_\nu(0) d\nu}. \quad (3)$$

When the emission and absorption profiles are considered to have identical and purely Doppler-broadened line shapes, integration of Eq. (3) is easily performed in the form of an infinite series:

$$G(k_0 x) = \sum_{n=0}^{\infty} \frac{(-k_0 x)^n}{n! \sqrt{(n+1)}}. \quad (4)$$

In the derivation of oscillator strengths from a comparison of the transmission as given by Eq. (4), with experimental results, two questions have to be answered:

(i) How far is the analysis applicable to the present experiment in view of the assumptions made in the derivation of the transmission function?

(ii) Is it possible to measure the relevant quantities, notably the number densities, with sufficient accuracy?

The condition of identical emission and absorption profiles has to do with the manner of excitation of the atoms. In the case of impact excitation, the emission profile may depart from the absorption profile due to recoil effects. In our previous work (I), the same transmission functions were found (within the accuracy of the experiment) for the $1^1S \rightarrow 2^1P$ helium transition for excitation by 40 and 1000 eV electrons. This result suggests that recoil effects do not influence the absorption measurements significantly. In the Appendix, a derivation of the recoil-velocity distributions for helium atoms is presented using differential excitation cross sections calculated in the first Born approximation. From a convolution of the recoil-velocity distribution with the Doppler-velocity distribution of the helium atoms at room temperature, the emission profile of the excited atoms is found. To check possible recoil effects on the transmission function, a numerical integration of Eq. (3) was performed for various convoluted emission profiles. From the first-Born-approximation results for the 2^1P excitation of helium by 150 eV electrons, it was found that the recoil influences the transmission function negligibly (effects on the oscillator strengths derived are much smaller than 1%). In Fig. 1, we show the transmission function for the unrealistic case of isotropic scattering of 60 eV electrons on helium. In this case, the oscillator strengths derived would be about 5% too low. For illustrative purposes, we give in the insert of Fig. 1 the transmission function using the recoil-velocity distribution obtained when assuming that the differential cross section resembles that of the 3^1S excitation of helium at 150 eV. This calculation is of interest for neon and argon resonance levels because the differential cross section might be less peaked in the forward direction than for the helium resonance levels. The calculation of the differential cross section was performed in the first Born approximation. Effects on the oscillator strengths obtained would be less than 2% in this case. We conclude, therefore, that even for a light atom the influence of recoil effects on the derived oscillator strengths is negligible. This conclusion should also hold for resonance

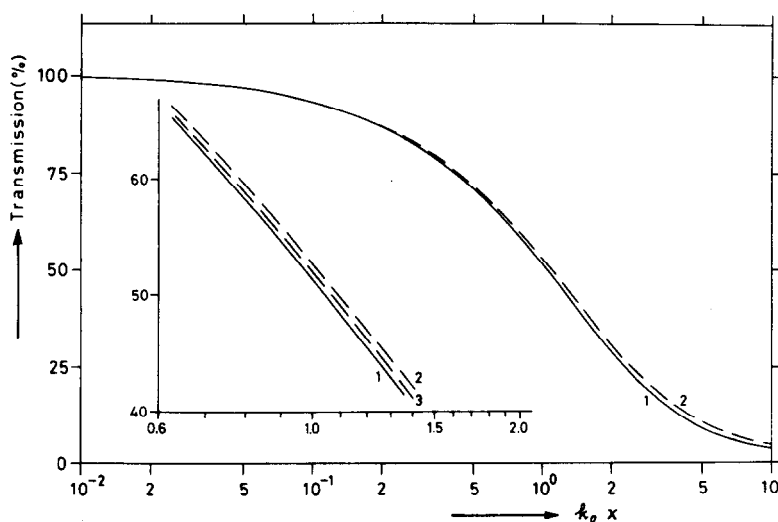


Fig. 1. Calculated transmission of a resonance line as a function of the reduced gas pressure ($k_0 x$), and its modification by recoil broadening of the emission line profile [Eq. (3)]. The absorption profile was considered to be a purely Doppler profile, according to the gas temperature [see Eq. (1)]. Curve 1: identical emission and absorption profiles. Curve 2: the emission profile broadened by recoil of the excited atoms due to the exciting collisions: in this example isotropic scattering of 60 eV electrons on helium (transferring 21 eV in the collision) has been taken into account. In curve 3 (see insert, with expanded scales), recoil effects are taken into account for scattering of 150 eV electrons on helium, assuming a forwardly peaked differential cross section, which resembles the excitation of the 3^1S level (in the first Born approximation). Curve 3 almost coincides with the case of isotropic scattering of 40 eV electrons (transferring 21 eV in the collision). No corrections for polarized emission (see the Appendix) were applied in these cases.

transitions of the heavier rare gases. Recoil velocities are inversely proportional to the mass of the excited atom whereas the r.m.s. Doppler velocities are inversely proportional to the *square root* of the atom mass. A point only briefly mentioned in I concerns the departure from a purely Doppler-broadened line shape (according to the gas temperature) due to the finite lifetime of the levels involved (natural broadening). As a consequence of natural broadening we must deal with a Voigt profile, which is the convolution of the Doppler line shape with a Lorentzian line shape. The frequency-dependent absorption coefficient $k_V(\nu)$ for a Voigt line profile is given by

$$k_V(\nu) = k_0 \frac{\alpha}{\pi} \int_{-\infty}^{\infty} \frac{\exp(-v^2) dv}{\alpha^2 + (w - v)^2}, \quad (5)$$

where

$$\alpha = \frac{c\Gamma}{4\pi\nu_0} \sqrt{\left(\frac{M}{2k_B T}\right)}, \quad (6)$$

$$w = \frac{c(\nu - \nu_0)}{\nu_0} \sqrt{\left(\frac{M}{2k_B T}\right)}, \quad (7)$$

with Γ representing the radiative decay constant. The parameter α (natural damping ratio) is proportional to the ratio of the FWHM of the Lorentz profile and the Doppler profile. Calculations were performed to evaluate the transmission function by numerical integration of Eq. (3) using identical Voigt profiles for the emission and absorption lines. In these calculations, the fast computing method of PIERLUISSI *et al.*^(13a) was used to perform the integration of Eq. (5) [see also VAN DER HELD^(13b) and ARMSTRONG^(13c)]. The calculated transmission functions are shown in Fig. 2 for a range of natural damping ratios α . The largest values for the parameter α encountered in the present experiments are of the order of 0.01 (for the neon resonance line at 73.6 nm and the argon resonance line at 104.8 nm). In the range of weighted absorption lengths $k_0 x$ considered in these experiments this means, that even for (these two) strong resonance lines the influence on the oscillator strengths derived is smaller than 2%. For the weaker lines the results are not affected by more than 1%.†

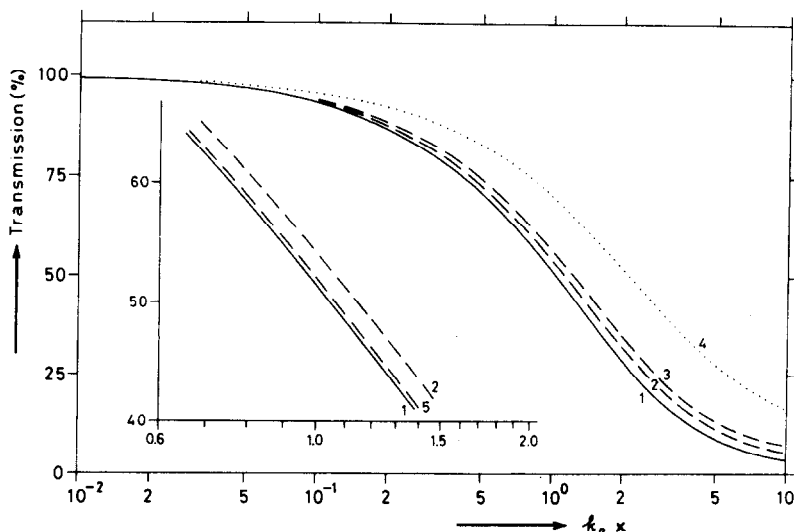


Fig. 2. Transmission functions (compare Fig. 1) calculated by numerical integration of Eq. (3) for the case of identical Voigt profiles [Eq. (5)] for the emission and absorption profile. Curve 1: $\alpha = 0$; curve 2: $\alpha = 0.05$; curve 3: $\alpha = 0.10$; curve 4: $\alpha = 0.50$; in the insert (with expanded scales), a detailed view is given for the value $\alpha = 0.01$ (curve 5), which is applicable in our case.

†In the range of pressures considered in these experiments, the effects of pressure broadening are much smaller [see, for instance, LEWIS⁽²³⁾ where the self-broadening constants for several rare gas transitions are given].

The quantities important in the absorption process are the temperature T , the absorption length x and the number density $n(p)$ of the atoms at the pressure p [see Eqs. (2) and (4)]. Although the gas is introduced in the excitation chamber at room temperature, it is *a priori* not certain whether the velocity distribution remains in accordance with room temperature. The heat input of the cathode, for instance, causes the scattering cell to rise in temperature to about 50°C. Absorption measurements were therefore carried out with a water-cooled scattering cell and compared with measurements taken with an uncooled cell. No differences were found between the two measurements. It was, therefore, concluded that the velocity distribution of the atoms corresponds to room temperature.

The absorption length is obtained geometrically as the distance between the scattering cell and the entrance slit of the v.u.v. spectrometer. However, a (small) correction has to be applied for absorption in the spectrometer. In I, this correction was obtained from the known pumping speed in the spectrometer and by calculating the gas flow through the entrance slit from the known width and height. To check this approach, absorption measurements were made for the He ($1^1S \rightarrow 2^1P$) transition at various slitwidths. From a linear extrapolation of the oscillator strengths obtained to zero slitwidth, correction factors for finite slitwidths were derived, which were in agreement with the calculated corrections. For the heavier rare gases, these corrections are much smaller than for helium because of the smaller conductance of the slit system for the heavier gases. The effective pumping speed, which is achieved in the spectrometer, is almost independent of the atomic mass in the range of masses considered here. The corrections depend on the slit widths used and are of the order of $(5 \pm 1)\%$ or less for the present experiments.

In the derivation of *absolute* values for oscillator strengths, an important problem concerns the determination of atomic number densities which usually limits the ultimate accuracy to be obtained. An exception is formed by the method employed by Penkin and coworkers where the absolute determination of number densities is circumvented by combining the hook method of Rozhdestvenskii with a total absorption measurement.^(14,15) In contrast, the determination of lifetimes depends only on the generation of absolute time scales which may be obtained very accurately [see, e.g. ASTNER *et al.*⁽¹⁶⁾]. In the present work, an ionization gauge was used to determine the *relative number densities*. Conversion to absolute scale was accomplished by *absolute pressure* measurements with a capacitance manometer. The comparison of ionization manometer and capacitance manometer readings was performed *in situ* and repeated regularly.

As to the final accuracy to be obtained for the atom number densities several factors are of importance:

(a) The variation of the number density along the absorption path should be negligibly small. It was verified that this is indeed the case by comparing measurements under flowing gas conditions with measurements under static conditions (only a small flow was maintained through the slit system by the pumping action in the spectrometer; the background pressure in the excitation chamber was kept in the 10^{-5} Pa range by means of getter pumps). No differences were found between these two cases.

(b) Another point concerns the absolute accuracy of the capacitance manometer. Capacitance manometers have been tested extensively in the last few years.^(17,18) It was found that commercial capacitance manometers are accurate to better than 2% for pressures down to 5×10^{-2} Pa. For reasons of stability, the capacitance manometer we used was kept at a temperature of 51°C. Therefore, a correction factor of 1.04 for the thermal transpiration effect should be taken into account [see DUSHMAN⁽¹⁹⁾]. This correction was not applied to the results presented in I; therefore, the oscillator strengths given in I should be multiplied by 1.04 (see Tables 1 and 2).

(c) The ionization gauge used is of the Bayard-Alpert type. The response of the device should be linear with density up to about 10^{-1} Pa (at room temperature). It is difficult to check accurately the linearity outside the range where a meaningful comparison with the capacitance manometer is possible, but the measurements presented in I on the helium $1^1S \rightarrow 2^1P$ transition, which can be compared with very accurate calculations,⁽⁷⁾ gave us confidence in the reliability of the gauge. However, at a later stage of this work, departures from linearity entered, as was shown from small changes in the shape of the experimental transmission functions (resulting in changes of up to 10% in the oscillator strengths obtained). These changes were strongest for helium, much less for neon and absent for argon. By changing the grid potential of the

Table 1. Absorption oscillator strengths f (in units 10^{-3}) of neon for transitions from the ground state $(2p^6)^1S$ to the resonance levels $1s_2$ and $1s_4$ (Paschen notation).

Upper level:				
j-K coupling	$3s [3/2]_1$	$3s' [1/2]_1$		
Paschen	$1s_4$	$1s_2$		
Wavelength (nm)	74.37	73.59		
Energy (eV)	16.67	16.85		
AUTHORS:	$10^3 \times f$	$10^3 \times f$	Ratio($1s_2/1s_4$)	EXPERIMENTAL METHODS
<i>present</i>	10.9 ± 0.9	147 ± 12	13.5	Absolute selfabsorption.
<i>paper I</i> ($\times 1.04$)	10.3 ± 0.8	147 ± 11	14.3	Absolute selfabsorption.
<i>De Jongh and Van Eck</i> ⁽²¹⁾	—	134 ± 10	—	Relative selfabsorption.
<i>NBS</i> [†]	12 ± 1	154 ± 16 [‡]	12.8	Forward inelastic electron scattering (400 eV).
<i>Geiger</i> ⁽²²⁾	9 ± 2	131 ± 26	14.5	Forward inelastic electron scattering (30 keV).
<i>Lewis</i> ⁽²³⁾	12 ± 2	168 ± 20	14.0	Pressure broadening.
<i>Korolev et al</i> ⁽²⁴⁾	—	160 ± 14	—	Natural broadening.
<i>Lawrence and Liszt</i> ⁽²⁵⁾	7.8 ± 0.4	130 ± 13	16.7	Exponential decay (pulsed electron beam). Beam foil.
<i>Irwin et al</i> ⁽²⁶⁾	—	158 ± 6	—	Beam foil.
<i>Knyštautas and Drouin</i> ⁽²⁷⁾	7.8 ± 0.8	161 ± 11	20.6	Beam foil.
<i>Bhasker and Lurio</i> ⁽²⁸⁾	12.2 ± 0.9	148 ± 14	12.1	Cascade level crossing.
<i>Kazantsev and Chaika</i> ⁽²⁹⁾	13.8 ± 0.8	—	—	Relaxation of hidden alignment in a magnetic field.
CALCULATIONS				
<i>Semenov and Strugach</i> ⁽³⁰⁾	—	—	13.27	Experimental term splittings.
<i>Stewart</i> ⁽³⁵⁾	—	159		Time dependent Hartree-Fock.
<i>Albat and Gruen</i> ⁽³⁴⁾	11.3	149		Hartree-Fock (many configurations).
<i>Gold and Knox</i> ⁽³¹⁾	11 / 12	110 / 121		Hartree-Fock (ab initio/semi-empirical).
<i>Gruzdev and Loginov</i> ⁽³³⁾	10.6	139		Hartree-Fock (many configurations).
<i>Aymar et al</i> ^{(32)§}	$L: 7.6; v: 10.4$	$L: 102; v: 135$		Parametrized potential (first order)
	12.1; 10.0	161; 130		— (second order).

[†] Unpublished data of *Kuyatt, Mielczarek and Natali*; private communication with Dr. C. E. Kuyatt (1977).

[‡] Slightly changed from the value quoted in Ref. 36.

§ Transition integrals calculated in both $L(ength)$ and $v(elocity)$ formulation.

ionization gauge from 180 to 100 V (with respect to ground potential), this problem could be completely eliminated. As an explanation, we suggest secondary electron emission from the collector due to ion impact. The helium ions with their relatively high velocities are probably much more effective in this process than neon or argon ions.^(20a,b) The process of secondary electron emission depends critically on the surface conditions of the collector and may affect the linearity of the gauge.

Concerning the final accuracy obtained for the oscillator strengths, we refer to the discussion given in I.

3. MEASUREMENTS AND RESULTS

The apparatus used in the present investigation has been described in I and only a few modifications were introduced. The observations reported in I were made at an emission angle at 55° with the electron beam whereas in this work the electron beam was viewed at right angles. (The orientation of the plane formed by the electron beam and the direction of observation was kept, as in I, at an angle of 45° with respect to the entrance slit of the spectrometer. In this way, a change in the degree of polarization of the observed radiation should not influence the results.) We changed the direction of observation to make the recoil calculations presented in the Appendix directly applicable to the experimental situation. The apparatus was further equipped with a quadrupole mass spectrometer to verify the purity of the gas.

Table 2. Absorption oscillator strengths f (in units 10^{-3}) of neon for transitions from the ground state $(2p^6)^1S$ to a number of higher lying resonance levels.

Upper level:		$4s\ 1/2\ 1_1$		$4s\ 1/2\ 1_1$		$5s\ 1/2\ 1_1$		$5s\ 1/2\ 1_1$		$3d\ 3/2\ 1_1$	
j-K coupling		$2s_2$		$2s_2$		$3s_2$		$3s_2$		$3s_1$	
Paschen		62.97		62.68		60.27		60.00		61.56	
Wavelength (nm)		19.69		19.78		20.57		20.66		20.14	
Energy (eV)		$10 \times f$		$10 \times f$		$10 \times f$		$10 \times f$		$10 \times f$	
AUTHORS:		Ratio($2s_2/2s_1$)		Ratio($3s_2/3s_1$)		Ratio($3s_2/3s_1$)		Ratio($3s_2/3s_1$)		Ratio($3s_2/3s_1$)	
<i>present</i>		12.8 \pm 1.0		15.3 \pm 1.2		1.20		4.2 \pm 0.3		0.69	
<i>paper I</i> ($\times 1.04$)		12.4 \pm 1.2		14.7 \pm 1.3		1.19		5.7 \pm 0.6		—	
NBS^\dagger		13 \pm 1		16 \pm 1		1.23		6.3 \pm 0.6		0.68	
<i>Geiger</i> [‡]		10.5		11.0		1.05		5.7		0.44	
<i>Decombe and Dumont</i> (38)		—		16.4 \pm 2.0		—		—		—	
<i>Ducloy</i> (39)		—		15.3 \pm 3.0		—		—		—	
<i>Klose</i> (40)		—		—		—		4.0 \pm 0.3		—	
<i>Lawrence and Liszt</i> (25)		13.4 \pm 1.0 [§]		17.8 \pm 2.5 [§]		1.33		6.2 \pm 1.0 [§]		0.77	
		(8.6 \pm 1.0)		(13.0 \pm 2.0)		(1.55)		(5.7 \pm 1.0)		(0.74)	
<i>Semenov and Strugach</i> (30)		—		—		1.28		—		0.726	
<i>Gruzdev and Logvinov</i> (33) [¶]		12.1		16.4		—		4.6		8.1	
<i>Klose</i> (41)		—		15.6		—		—		—	
		—		—		—		—		—	
		—		—		—		—		—	
		—		—		—		—		—	
		—		—		—		—		—	
		—		—		—		—		—	
		—		—		—		—		—	
		—		—		—		—		—	
		—		—		—		—		—	
		—		—		—		—		—	
		—		—		—		—		—	
		—		—		—		—		—	
		—		—		—		—		—	
		—		—		—		—		—	
		—		—		—		—		—	
		—		—		—		—		—	
		—		—		—		—		—	
		—		—		—		—		—	
		—		—		—		—		—	
		—		—		—		—		—	
		—		—		—		—		—	
		—		—		—		—		—	
		—		—		—		—		—	
		—		—		—		—		—	
		—		—		—		—		—	
		—		—		—		—		—	
		—		—		—		—		—	
		—		—		—		—		—	
		—		—		—		—		—	
		—		—		—		—		—	
		—		—		—		—		—	
		—		—		—		—		—	
		—		—		—		—		—	
		—		—		—		—		—	
		—		—		—		—		—	
		—		—		—		—		—	
		—		—		—		—		—	
		—		—		—		—		—	
		—		—		—		—		—	
		—		—		—		—		—	
		—		—		—		—		—	
		—		—		—		—		—	
		—		—		—		—		—	
		—		—		—		—		—	
		—		—		—		—		—	
		—		—		—		—		—	
		—		—		—		—		—	
		—		—		—		—		—	
		—		—		—		—		—	
		—		—		—		—		—	
		—		—		—		—		—	
		—		—		—		—		—	
		—		—		—		—		—	
		—		—		—		—		—	
		—		—		—		—		—	
		—		—		—		—		—	
		—		—		—		—		—	
		—		—		—		—		—	
		—		—		—		—		—	
		—		—		—		—		—	
		—		—		—		—		—	
		—		—		—		—		—	
		—		—		—		—		—	
		—		—		—		—		—	
		—		—		—		—		—	
		—		—		—		—		—	
		—		—		—		—		—	
		—		—		—		—		—	
		—		—		—		—		—	
		—		—		—		—		—	
		—		—		—		—		—	
		—		—		—		—		—	
		—		—		—		—		—	

3.1 Neon

Measurements for neon were carried out, in part, with pure ^{20}Ne gas and partly with a natural mixture of ^{20}Ne and ^{22}Ne . We have verified that the isotope shift between the resonance lines of ^{20}Ne and ^{22}Ne is so small in comparison to the Doppler widths of the lines that the oscillator strengths derived are not influenced by the isotope shift. Consequently, the results given for the oscillator strengths of the neon resonance lines in I should be correct, apart from the factor 1.04 which accounts for the thermal transpiration effect (see Section 2). The lines originating from the two lowest lying resonance levels (73.6 and 74.4 nm) were resolved in the first-order spectrum and the other lines in the second-order spectrum. Electron-beam energies ranged from 60 to 100 eV. An example of an absorption measurement is given in Fig. 3. The oscillator strengths derived are given in Tables 1 and 2.

For transitions to the two lowest lying resonance levels (the Paschen $1s_2$ and $1s_4$ levels), a relatively large amount of data is available, both experimentally and theoretically (Table 1). For the $1s_2$ level, our results are within error limits in agreement with the other results listed. However, the lowest values quoted for the transition to the $1s_2$ level [DE JONGH and VAN ECK,⁽²¹⁾ GEIGER,⁽²²⁾ and LAWRENCE and LISZT⁽²⁵⁾] depart considerably from the highest values (LEWIS,⁽²³⁾ KOROLEV *et al.*,⁽²⁴⁾ IRWIN *et al.*,⁽²⁶⁾ and KNYSTAUTAS and DROUIN⁽²⁷⁾). For the $1s_4$ level, the two extremes are the results of LAWRENCE and LISZT⁽²⁵⁾ and of KNYSTAUTAS and DROUIN⁽²⁷⁾ on the low side and on the high side the result of KAZANTSEV and CHAIKA,⁽²⁹⁾ they differ by more than a factor of 1.5. The calculations are mostly semi-empirical in that, at a certain stage of the calculations, experimental term values are used. The more recently calculated oscillator strengths show less spread than the experimental values. In Table 1, we also give the ratio of the oscillator strengths for the two transitions as obtained by different authors. This ratio has been calculated by SEMENOV and STRUGACH⁽³⁰⁾ from experimental term splittings using the one-configuration approximation. The agreement with the experimental values [except those of LAWRENCE and LISZT⁽²⁵⁾ and those of KNYSTAUTAS and DROUIN⁽²⁷⁾] shows that configuration interaction is not very important. The oscillator strengths given in Refs. (25) and (27) for the transition to the $1s_4$ level appear too low.[†]

The results for the higher resonance levels are given in Table 2. We derived oscillator strengths from the life-time results of LAWRENCE and LISZT⁽²⁵⁾ by using theoretical branching ratios obtained from the results of Refs. (33), (37), and (42). The spread in the experimental

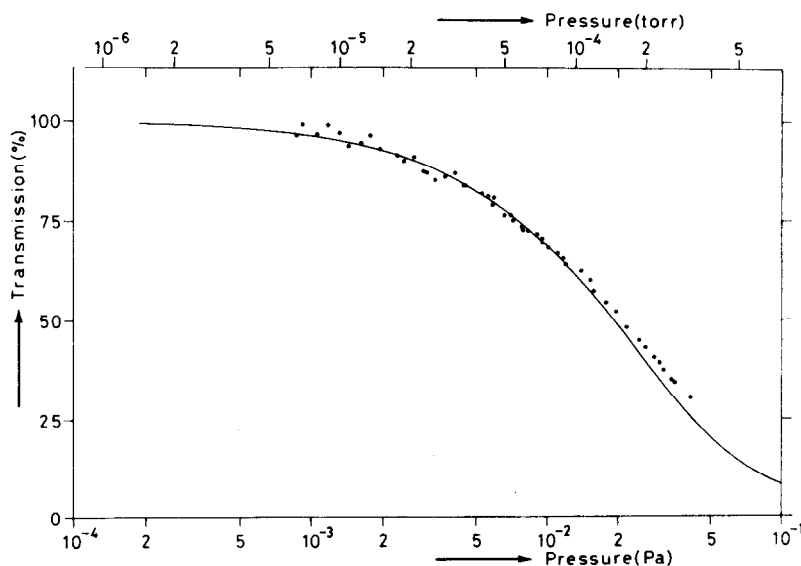


Fig. 3. The experimental transmission function obtained for the neon transition $3s[3/2]_1 \rightarrow (2p^6)^1S$ (74.4 nm). The solid line agrees with curve 1 of Fig. 2 and represents the fit which was used in the derivation of the oscillator strength (result: $f = 10.9 \times 10^{-3}$, see Table 1).

[†]The influence of cascading on the exponential decay curves of the neon and argon $1s_4$ level is particularly severe. This may explain the low oscillator strengths of Refs. (25) and (27).

values is remarkably small in comparison with the results of Table 1. The calculations show reasonable agreement with the experimental values. Ratios of oscillator strengths are given for transitions to the $2s_2$ and $2s_4$ levels and for the transitions to the $3s_2$ and $3s_4$ levels, which are in good agreement with the results of SEMENOV and STRUGACH⁽³⁰⁾ as derived from term splittings.

3.2 Argon

The measurements on the argon transitions were carried out in the first-order spectrum. A problem with these transitions is the overlap with Ar(II) and Ar(III) lines in the second- and third-order. To eliminate contributions of these higher-order lines, it is necessary to choose the energy of the exciting electrons sufficiently low. The energies used in the measurements on the argon transitions were in the range 20–45 eV. For measurements at relatively high pressures, as for the $3d_5$ (Paschen) level, the space charge of the ions formed causes a pressure-dependent shift of the actual excitation energies. At a pressure of 10^{-1} Pa, this shift was found to be about 3 eV when electron currents of 40 μ A were used at 30 eV. The shift was obtained from the displacement of the excitation threshold of the Ar(II) line at 92 nm. Therefore, the energies were chosen such that the variation of the excitation cross section with energy is small. For the $3d_5$ level, which has a strong triplet character, a beam energy of 20 eV was used (see the insert of Fig. 4) and the pressure measurements were in part carried out directly with the capacitance manometer. An absorption measurement is shown in Fig. 4. The results are given in Tables 3 and 4.

Results for the two lowest lying resonance levels are given in Table 3. The remarks made on the ratio of the oscillator strengths for the two lowest lying resonance levels of neon also apply to the ratio of argon oscillator strengths. The calculations by LEE and LU⁽⁵¹⁾ and by LEE⁽⁵²⁾ are carried out using a multi-channel quantum-defect treatment (MQDT). In the MQDT theory, the configuration interactions between the different Rydberg series are accounted for. The accuracy of this method for low-lying levels is not expected to be very good but, for higher lying states of heavier rare gases where configuration interaction is important, better results are obtained.

Results for the higher lying resonance levels of argon are given in Table 4. The data for these transitions are scarce. Our values are, on the average, about 10% lower than the other experimental values listed in Table 4. The results of the calculations show in some cases large departures from the experimental values, illustrating the effects of configuration interaction.

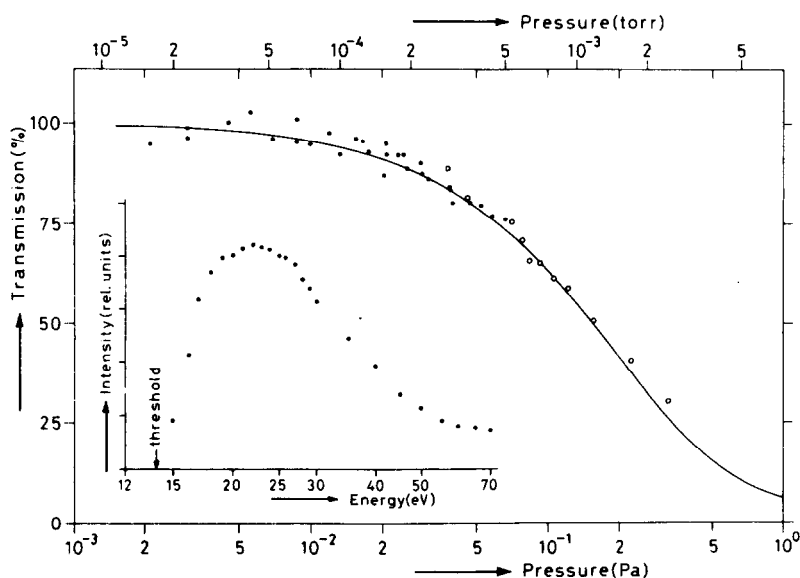


Fig. 4. The experimental transmission function obtained for the argon transition $3d[\frac{1}{2}]_1 \rightarrow (3p^6)^1S$ (89.4 nm): ● data obtained using the ionization manometer, ○ data obtained by direct measurement with the capacitance manometer. An electron-beam energy of 20 eV was used in the determination of the transmission function. The solid line represents the fit which was used in the derivation of the absorption oscillator strength (result: $f = 0.89 \times 10^{-3}$, see Table 4). In the insert, a part of the excitation function $(3p^6)^1S \rightarrow 3d[\frac{1}{2}]_1$ is given (this result was obtained at a pressure of 10^{-2} Pa and electron currents of 20 μ A).

Table 3. Absorption oscillator strengths f (in units 10^{-3}) of argon for transitions from the ground state $(3p^6)^1S$ to the resonance levels $1s_2$ and $1s_4$ (Paschen notation).

Upper level:				
j-K coupling	$4s\ 1\ 3/2\ 1_1$	$4s\ 1\ 1/2\ 1_1$		
Paschen	$1s_4$	$1s_2$		
Wavelength (nm)	106.67	104.82		
Energy (eV)	11.62	11.83		
	$10 \times f$	$10 \times f$	Ratio($1s_2/1s_4$)	
AUTHORS:				EXPERIMENTAL METHODS
<i>present</i>	63 ± 5	240 ± 20	3.81	Absolute selfabsorption.
<i>De Jongh and Van Eck</i> ⁽²¹⁾	—	220 ± 20	—	Relative selfabsorption.
NBS [†]	$67 \pm 7^{\S}$	$267 \pm 28^{\S}$	3.98	Forward inelastic electron scattering (400 eV).
<i>Geiger</i> [‡]	66	255	3.86	Forward inelastic electron scattering (30 keV).
<i>Lewis</i> ⁽²³⁾	63 ± 4	278 ± 20	4.40	Pressure broadening.
<i>Copley and Camm</i> ⁽⁴³⁾	76 ± 8	283 ± 24	3.72	Pressure broadening.
<i>Vallee et al</i> ⁽⁴⁴⁾	51 ± 7	210 ± 30	4.12	Pressure broadening.
<i>Lawrence</i> ⁽⁴⁵⁾	59 ± 3	228 ± 21	3.87	Exponential decay (pulsed electron beam).
<i>Irwin et al</i> ⁽⁴⁶⁾	83 ± 27	350 ± 130	4.22	Beam foil.
				CALCULATIONS
<i>Semenov and Strugach</i> ⁽³⁰⁾	—	—	4.13	Experimental term splittings.
<i>Lee and Lu</i> ⁽⁵¹⁾	80	210		Multi-channel quantum defect (semi-empirical).
<i>Lee</i> ⁽⁵²⁾	59	300		Multi-channel quantum defect (ab-initio).
<i>Stewart</i> ⁽⁵⁰⁾	—	270		Time dependant Hartree-Fock.
<i>Albat et al</i> ⁽⁴⁹⁾	48	188		Hartree-Fock.
<i>Knox</i> ⁽⁴⁷⁾	52 / 49	170 / 200		Hartree-Fock (ab-initio/semi-empirical).
<i>Grushev and Loginov</i> ⁽⁴⁸⁾	61	231		Hartree-Fock (many configurations).
<i>Aymar et al</i> ^{(32)¶}	1:53 ; ν :59	1:210 ; ν :226		Parametrized potential (first order)
	71 ; 65	286 ; 252		— (second order).

[†] Unpublished data of *Kuyatt, Mieloszarek and Natali*; private communication with Dr.C.E.Kuyatt (1977).

[‡] Unpublished data; private communication with Prof.Dr.J.Geiger (1978).

[§] Slightly changed from the value quoted in Ref.52.

[¶] Transition integrals calculated in both $L(\text{length})$ and $\nu(\text{velocity})$ formulation.

These effects are also clear when we compare the ratio of oscillator strengths for the transitions to the $2s_2$ and $2s_4$ levels. The result of SEMENOV and STRUGACH,⁽³⁰⁾ which was derived from experimental term splittings by using the one-configuration approximation, is clearly in error for this case.

4. CONCLUDING REMARKS

Remarkable good agreement exists between the present optical results and the results from forward inelastic electron scattering. In particular, our results agree with the NBS results to well within the error limits except for one case (the transition to the $3s_1$ level of argon). This fact illustrates the power of deriving oscillator strengths from electron-scattering data although, in some cases, considerable care is required to carry out the extrapolation to zero transfer of momentum in the excitation process [see LASSETTRE and SKERBELE⁽¹²⁾].

The accuracy of the present method may be improved, particularly the determination of the number densities and the absorption length. The path length in the spectrometer may be reduced by using a grazing incidence spectrometer, resulting in smaller corrections on the absorption length at comparable wavelength resolution. With the apparatus optimized for the present method, it should be possible to derive oscillator strengths with an accuracy of better than 5%.

The present method may be extended to transitions involving resonance states with higher principal quantum numbers than are covered in the present work (provided sufficient wavelength resolution is obtained in the v.u.v. spectrometer).

Of particular interest are the effects of configuration interaction. For the heavier rare gases,

Table 4. Absorption oscillator strengths f (in units 10^{-3}) of argon for transitions from the ground state $(3p^6)^1S$ to a number of higher lying resonance levels.

Upper level: j-k coupling	5s (3/2) 1	5s (1/2) 1	3d (1/2) 1	3d (3/2) 1	3d (3/2) 1
Paschen	2s ₂	2s ₂	3d ₂	3d ₂	3s ₁
Wavelength (nm)	87.99	86.98	89.43	87.61	86.68
Energy (eV)	14.09	14.26	13.86	14.15	14.30
AUTHORS:					
present	$10 \times f$	$10 \times f$	Ratio(2s ₂ /2s ₁)	$10 \times f$	$10 \times f$
NBS†	25 ± 2	10.6 ± 0.8	0.42	79 ± 6	86 ± 7
Geiger‡	28 ± 3	12.4 ± 4	0.44	92 ± 9	110 ± 11
Lawrence (45)	32	10.8	0.34	108	97
	27 ± 2	13 ± 3	0.48	93 ± 6	107 ± 15
EXPERIMENTAL METHODS					
					Absolute selfabsorption.
					Forward inelastic electron scattering (400 eV).
					Forward inelastic electron scattering (30 keV).
					Exponential decay (pulsed electron beam).
CALCULATIONS					
					Experimental term splittings.
					Multi-channel quantum defect (semi-empirical).
					Multi-channel quantum defect (ab-initio).
					Hartree-Fock (geometric mean of λ and ν results).
					Parametrized potential.
					Parametrized potential (first order) (configuration interaction).
Semenov and Strugach (30)			0.78		
Lee and Lu (51)	45	39	1.6	45	128
Lee (52)	34	25	1.1	53	110
Grunder and Logvinov (48)§	29	24	4.6	88	350
Aymar and Schweighofer (54)¶	1:36 ; ν :37	1:12.6 ; ν :12.0	1:3.8 ; ν :4.5	1:286 ; ν :302	1:417 ; ν :417
Aymar (53)¶	28.2 ; 30.0	21.7 ; 22.7			
	34.4 ; 36.7	11.1 ; 11.5			

† Unpublished data of Kuyatt, Melozavok and Natali; private communication with Dr. C.E. Kuyatt (1977).

‡ Unpublished data; private communication with Prof. Dr. J. Geiger (1978).

§ Calculated lifetimes converted to oscillator strengths using transition probabilities of Izilly (55).

¶ Transition integrals calculated in both $l(\text{length})$ and $\nu(\text{velocity})$ formulation.

these effects become more and more pronounced. However, application of the present method to krypton or xenon transitions will probably necessitate the use of pure isotopes. The broader applicability of the electron scattering method becomes evident in these cases, where the unknown line shapes complicate the interpretation of optical absorption measurements.

Acknowledgements—The authors are indebted to Dr. C. E. KUYATT (N.B.S. Washington D.C.) and to Prof. J. GEIGER (University of Kaiserslautern) for allowing us to quote their unpublished results. Discussions with Prof. J. A. SMIT and with Dr. H. G. M. HEIDEMAN are gratefully acknowledged. This work was performed as part of the research program of the "Stichting voor Fundamenteel Onderzoek der Materie" (F.O.M.) with financial support from the "Nederlandse Organisatie voor Zuiver Wetenschappelijk Onderzoek" (Z.W.O.).

REFERENCES

1. J. COOPER, *Rep. Progr. Phys.* **29**, 35 (1966).
2. R. W. P. MCWHIRTER in *Plasma Diagnostic Techniques* (Edited by R. H. HUDDLESTONE and S. L. LEONARD), Chap. 5. Academic Press, New York (1965).
3. C. BRETON and J. L. SCHWOB, in *Some Aspects of Vacuum Ultraviolet Radiation Physics* (Edited by N. VODAMY, J. ROMAND, and B. VODAR), Chap. 8. Pergamon Press, Oxford (1974).
4. D. H. MENZEL (Ed.), *Selected Papers on Physical Processes in Ionized Plasmas*. Dover, New York (1962).
5. D. R. BATES and A. DAMGAARD, *Proc. Roy. Soc. A* **242**, 101 (1949).
6. H. A. BETHE and E. E. SALPETER, *Handbuch der Physik* **35**, 88 (1957).
7. B. SCHIFF, C. L. PEKERIS, and Y. ACCAD, *Phys. Rev. A* **4**, 885 (1971).
8. F. WEINHOLD, *J. Chem. Phys.* **54**, 1874 (1971).
9. M. T. ANDERSON and F. WEINHOLD, *Phys. Rev. A* **9**, 118 (1974).
10. H. G. BERRY, *Rep. Progr. Phys.* **40**, 155 (1977).
11. W. B. WESTERVELD and J. VAN ECK, *JQSRT* **17**, 131 (1977).
12. E. N. LASSETTRE and A. SKERBELE, in *Methods of Experimental Physics* (Edited by L. MARTON), Vol. 3B, p. 868. Academic Press, New York (1974).
- 13(a). J. H. PIERLUISSI, P. C. VANDERWOOD, and R. B. GOMEZ, *JQSRT* **18**, 555 (1977). (b) E. F. M. VAN DER HELD, *Z. Phys.* **70**, 508 (1931). (c) B. H. ARMSTRONG, *JQSRT* **7**, 61 (1967).
14. YU. I. OSTROVSKII and N. P. PENKIN, *Opt. Spektrosk.* **11**, 3 (1961) [*Opt. Spectrosc.* **11**, 1 (1961)].
15. W. C. MARLOW, *Appl. Opt.* **6**, 1715 (1967).
16. G. ASTNER, L. J. CURTIS, L. LILJEBY, S. MANNERNIK, and I. MARTINSON, *Z. Phys.* **A279**, 1 (1976).
- 17(a). N. G. UTTERBACK and T. GRIFFITH, *Rev. Sci. Instrum.* **37**, 866 (1966). (b) G. LORIOT and T. MORAN, *Rev. Sci. Instrum.* **46**, 140 (1975).
18. B. VAN ZIJL, *Rev. Sci. Instrum.* **47**, 1214 (1976).
19. S. DUSHMAN, *Scientific Foundations of Vacuum Technique* (Edited by J. M. LAFFERTY), 2nd Edn. Wiley, New York (1962).
- 20(a). M. KAMINSKY, *Atomic and Ionic Impact Phenomena on Metal Surfaces*, pp. 321–324. Springer Verlag, Berlin (1965). (b) L. A. DIETZ and J. C. SHEFFIELD, *J. Appl. Phys.* **46**, 4361 (1975).
21. J. P. DE JONGH and J. VAN ECK, *Physica* **51**, 104 (1971).
22. J. GEIGER, *Phys. Lett.* **33A**, 351 (1970).
23. E. L. LEWIS, *Proc. Phys. Soc.* **92**, 817 (1967).
24. F. A. KOROLEV, V. I. ODINTSOV, and E. V. FURSOVA, *Opt. Spektrosk.* **16**, 555 (1964) [*Opt. Spectrosc.* **16**, 304 (1964)].
25. G. M. LAWRENCE and H. S. LISZT, *Phys. Rev.* **178**, 122 (1969).
26. D. J. G. IRWIN, A. E. LIVINGSTON, and J. A. KERNAHAN, *Can. J. Phys.* **51**, 1948 (1973).
27. E. KNYSTAUTAS and R. DROUIN, *Astron. Astrophys.* **37**, 145 (1974).
28. N. D. BHASKAR and A. LURIO, *Phys. Rev. A* **13**, 1484 (1976).
29. S. KAZANTSEV and M. CHAIKA, *Opt. Spektrosk.* **31**, 510 (1971) [*Opt. Spectrosc.* **31**, 273 (1971)].
30. R. I. SEMENOV and B. A. STRUGACH, *Opt. Spektrosk.* **24**, 487 (1968) [*Opt. Spectrosc.* **24**, 258 (1968)].
31. A. GOLD and R. S. KNOX, *Phys. Rev.* **113**, 834 (1959).
32. M. AYMAR, S. FENEUILLE, and M. KLAPISCH, *Nucl. Instr. Meth.* **90**, 137 (1970).
33. P. F. GRUZDEV and A. V. LOGINOV, *Opt. Spektrosk.* **35**, 5 (1973) [*Opt. Spectrosc.* **35**, 1 (1973)].
34. R. ALBAT and N. GRUEN, *J. Phys.* **B7**, L9 (1974).
35. R. F. STEWART, *Molec. Phys.* **29**, 1577 (1975).
36. R. P. SAXON, *Phys. Rev. A* **8**, 839 (1973).
37. A. V. LOGINOV and P. F. GRUZDEV, *Opt. Spektrosk.* **37**, 817 (1974) [*Opt. Spectrosc.* **37**, 467 (1974)].
38. B. DECOMPS and M. DUMONT, *IEEE J. Quantum Elect.* **QE-4**, 916 (1968).
39. M. DUCLOY, *Ann. de Phys. Ser. 14* **t8**, 403 (1973–74).
40. J. Z. KLOSE, *Phys. Rev.* **188**, 45 (1969).
41. J. Z. KLOSE, *JQSRT* **9**, 881 (1969).
42. P. F. GRUZDEV and A. V. LOGINOV, *Opt. Spektrosk.* **39**, 817 (1975) [*Opt. Spectrosc.* **39**, 464 (1975)].
43. G. H. COPLEY and D. M. CAMM, *JQSRT* **14**, 899 (1974).
44. O. VALLEE, R. RANSON, and J. CHAPELLE, *JQSRT* **18**, 327 (1977).
45. G. M. LAWRENCE, *Phys. Rev.* **175**, 40 (1968).
46. D. J. G. IRWIN, A. E. LIVINGSTON, and J. A. KERNAHAN, *Nucl. Instr. Meth.* **110**, 111 (1973).
47. R. S. KNOX, *Phys. Rev.* **110**, 375 (1958).
48. P. F. GRUZDEV and A. V. LOGINOV, *Opt. Spektrosk.* **38**, 817 (1975) [*Opt. Spectrosc.* **38**, 464 (1975)].
49. R. ALBAT, N. GRUEN, and B. WIRSAM, *J. Phys.* **B8**, L82 (1975).
50. R. F. STEWART, *Molec. Phys.* **30**, 745 (1975).
51. C. M. LEE and K. T. LU, *Phys. Rev. A* **8**, 1241 (1973).
52. C. M. LEE, *Phys. Rev. A* **10**, 584 (1974).
53. M. AYMAR, *Physica* **57**, 178 (1972).

54. M. AYMAR and M. G. SCHWEIGHOFER, *Physica* **67**, 585 (1973).
 55. R. A. LILLY, *J. Opt. Soc. Am.* **66**, 245 (1976).
 56. Y. K. KIM and M. INOKUTI, *Phys. Rev.* **175**, 176 (1968).
 57. L. VRIENS and J. D. CARRIÈRE, *Physica* **49**, 517 (1970).
 58. F. A. KOROLEV and V. I. ODINTSOV, *Opt. Spektrosk.* **18**, 968 (1965) [*Opt. Spectrosc.* **18**, 547 (1965)].
 59. N. F. MOTT and H. S. W. MASSEY, *The Theory of Atomic Collisions*, 2nd Edn. Oxford University Press, London (1949).

APPENDIX: DERIVATION OF THE RECOIL VELOCITY DISTRIBUTIONS OF HELIUM ATOMS EXCITED BY ELECTRON IMPACT

The electron beam is considered to be incident along the positive z -axis (see Fig. A1). For simplicity, the direction of observation of the emitted radiation is chosen to be perpendicular to the electron beam (along the x -axis). The initial atom velocities are so small that the electron-atom scattering process is not influenced. Consequently, the recoil-velocity distribution (due to the scattering process) and the initial Doppler velocity distribution of the atoms are independent of each other. The final velocity distribution is found by convolution of these two distributions (see Section 2). In this treatment, we therefore consider the helium atoms to be at rest before interaction with electrons takes place. For an atom excited by electrons scattered in the direction (θ, ϕ) , we find (from energy and momentum conservation) for the recoil velocity component along the x -axis the following result:

$$v_x = -v_0 \sin \theta \cos \phi \quad (\text{A1})$$

with

$$v_0 = \frac{m}{M} \sqrt{\left(2 \frac{E_0}{m} (1 - E_r/E_0)\right)}, \quad (\text{A2})$$

where E_0 is the incident electron energy and E_r is the excitation energy of the atomic level (these equations are simplified using $m/M \ll 1$). The fraction of atoms with recoil velocity between v_x and $v_x + dv_x$ is equal to

$$g(v_x) dv_x = \frac{1}{\sigma_t} \int_C \sigma_d(\theta) \sin \theta d\theta d\phi. \quad (\text{A3})$$

Here σ_t is equal to the total cross section and $\sigma_d(\theta)$ is the differential cross section for the excitation process. The integration is performed along the circle C : $\sin \theta \cos \phi = -v_x/v_0$. The integral given in Eq. (A3) becomes much more tractable when the coordinate system is rotated over 90° around the y -axis, so that the z' -axis coincides with the original x -axis. This allows us to rewrite Eq. (A3) as

$$g(v_x) dv_x = \frac{2}{\sigma_t} \left(\int_0^\pi \sigma_d(\theta) d\phi' \right) dv_x \quad (\text{A4})$$

with

$$\cos \theta = \sqrt{[1 - (v_x/v_0)^2]} \cos \phi'. \quad (\text{A5})$$

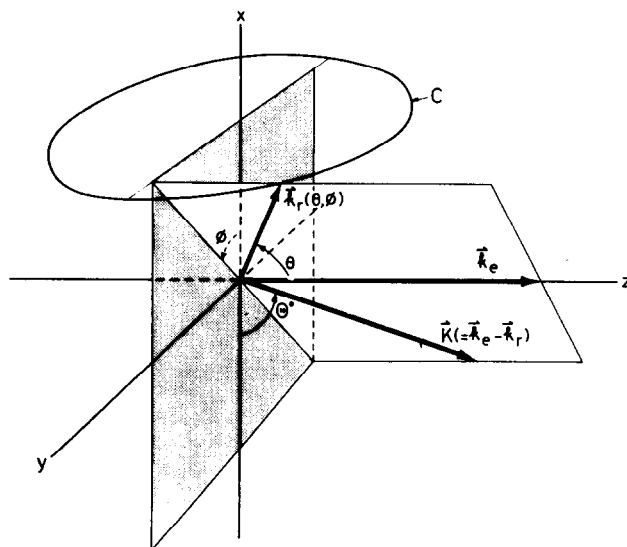


Fig. A1. The system of coordinate axes employed in the recoil-velocity calculations. An electron of momentum \mathbf{k}_e is incident along the z -axis. A helium atom at the origin of the coordinate system is excited by the incident electron, which is scattered in the direction (θ, ϕ) with final momentum \mathbf{k}_r . The momentum transferred to the atom in the collision process is given by $\mathbf{K} (= \mathbf{k}_e - \mathbf{k}_r)$. The angle θ^* indicated in the figure is the supplementary angle of θ , the angle between the momentum transfer vector \mathbf{K} and the direction of observation along the x -axis. The circle C indicates those electron-scattering directions which result in equal x -components of momentum transferred to the atom.

Table A1. The full width at half maximum height (in m/s) of the recoil-velocity distributions $g(v_x)$ [see Eq. (A4)] and $h(v_x)$ [a correction was applied for polarized emission, see Eq. (A9)], calculated in the Born approximation. Excitation of helium 1S and 1P states by electrons of energy E_0 is considered.

E_0 (eV)	3^1S		2^1P		3^1P
	$g(v_x)$	$g(v_x)^\dagger$	$g(v_x)$	$h(v_x)$	$h(v_x)^\dagger$
150	471	—	163	116	—
400	481	463	115	77	84
1000	488	—	82	53	—

† Calculation of Korolev and Odintsov (Ref. 58).

In the Born approximation, the differential cross section is given as

$$\sigma_d(\theta) = A[f(K)/K^2], \quad (\text{A6})$$

where A is a dimensionless constant, K is the momentum transferred in the collision (atomic units), and $f(K)$ is the generalized oscillator strength. † The dimensionless constant A is given by

$$A = \frac{4e^4 m^2 a_0^2 R k_r}{(4\pi\epsilon_0)^2 \hbar^4 E_r k_e}, \quad (\text{A7})$$

with a_0 the first Bohr radius of hydrogen, R the Rydberg energy and k_e and k_r the momenta of the incident and scattered electron, respectively. The relation between the momentum transfer K and the electron scattering angle θ follows from the cosine law, viz.

$$K^2 = k_e^2 + k_r^2 - 2k_e k_r \cos \theta. \quad (\text{A8})$$

Accurate calculations of $f(K)$ have been performed by KIM and INOKUTI⁽⁵⁶⁾ for a number of helium transitions. We used series expansions of the generalized oscillator strengths, as given by VRIENS and CARRIÈRE,⁽⁵⁷⁾ with parameters fitted to agree with the results of Ref. (56).

The velocity distribution given in Eq. (A4) cannot be used directly to give the frequency distribution of the radiation emitted when the radiation is polarized. In the Born approximation, the spatial intensity distribution of helium $^1P \rightarrow ^1S$ radiation is proportional to $\sin^2 \Theta$, where Θ is the angle between the direction of observation and K is the momentum transfer vector of the 1P excitation process. Consequently, when we introduce the (unnormalized) distribution $h(v_x)$ as

$$h(v_x) \sim \int_0^\pi \sigma_d(\theta) \sin^2 \Theta d\phi', \quad (\text{A9})$$

we obtain directly the frequency distribution of radiation emitted at right angles with respect to the electron beam by using

$$v_x = c[(\nu/\nu_0) - 1]. \quad (\text{A10})$$

Integration of Eqs. (A4) and (A9) was carried out numerically for excitation of the 2^1P and 3^1S state of helium. The full widths at half maximum of the calculated velocity distributions are given in Table A1 and compared with the calculation of KOROLEV and ODINTSOV.⁽⁵⁸⁾ The recoil-velocity distribution for excitation of the 3^1P state should be similar to the one obtained for the 2^1P state because the dependence of the differential cross section on the scattering angle is largely the same. KOROLEV and ODINTSOV⁽⁵⁸⁾ used the Born approximation, as given by MOTT and MASSEY.⁽⁵⁹⁾ It is clear that the two calculations agree reasonably well.

† In Fig. 2 of I, a mistake has been made. The maximum values of $(Ka_0)^2$ indicated for various electron energies must be shifted to higher values by one decade. The conclusions drawn in the text remain unchanged.